Structural, Optical, Electrical Studies on Pure and Irradiated Mannitol Single Crystals for Nonlinear Optical Applications

M. Priya[1,*], K. Sathyamoorthy[1], P. Vinothkumar[1], Ro. Mu. Jauhar[2], P. Murali Manohar[1], A. Selvam[3]

[1]Department of Physics, Saveetha Engineering College, Thandalam, Chennai 602 105, Tamil Nadu, India
[2]Department of Physics, VIT, Chennai 600 004, Tamil Nadu, India
[3]Department of Physics, Presidency College, Chennai, Tamil Nadu, India

***Corresponding author: E-mail: priyam7373@gmail.com**

DOI: 10.5185/amp.2020.010394

The Mannitol single crystal was grown by slow evaporation technique and irradiated by gamma radiation. Single crystal XRD analysis showed that irradiation not changed the crystal system. The crystalline perfection of pure and irradiated Mannitol single crystal were studied by high resolution X-ray diffraction analysis. The optical behaviour of pure and irradidated Mannitol was verified by the changes in the affected cut-off wavelength. The laser damage threshold was calculated for pure and irradiated Mannitol using laser source. The second harmonic generation of pure and gamma irradiated Mannitol were studied using Nd:YAG laser source and observed that SHG intensity decreases with increasing dose of gamma radiation.

Introduction

The nonlinear optical crystals has wide role in the area of science and technology and it is used in optoelectronics, photonics, optical modulation, second harmonic generation, optical signal processing, optical switching and optical data storage devices respectively [**1-3**]. The UV transmitter has been developed and made sustainable for ozone sensing applications based on space research [**4**]. The solid state lasers are used in orbital space mission instruments, space based light detection and ranging systems [**5**].

The space radiation can generate color centres and distraction of the applied coatings on bulk materials. The space instruments can be damaged by the exposure of space radiation. So it is essential to study the impact of radiation on the bulk material or laser applications materials [**6**]. Many researchers have developed and by giving importance to organic compound than inorganic by dosimetric methods. An organic amino acid based single crystal has been reported than inorganic materials for dosimetric application.

The ionizing radiation produces unpaired electrons without destroying the sample in the dosimetric technique. It is used in high dose rate measurements and industrial radiation applications. The irradiated materials can be used to know the radiation absorption and can be used in space device applications and dosimetric applications. Generally gamma radiation causes damage in bulk materials which leads to creation of Compton electrons and point defects thus resulting in altering its materials property respectively. Sometimes gamma ray interacts with non-crystalline materials by electronic ionization, electronic excitation and lead to separation of the orbital electrons [**7**].

The free electrons are produced within a material during penetration of radiation and they wander through the material. The foreign atom, an interstitial atom, a vacancy or any other imperfection in the structure causes irregularities in the material during the irradiation of gamma rays. The transparent inorganic material absorbs the radiations and 'color centers' are formed by the combination of the electron with the trapping site [**8**], where two condition can be considered. First, the center is stable due to tight bounding between electrons and the impurity or defect. Second, the center is weak because the electron is ready to escape from the trap and return to its positions in the solid.

Materials and methods

The commercial available Mannitol was purchased from Sigma Aldrich (99 %) and dissolved in methanol. The saturated solution was prepared and kept without disturbance. After 7 days, the colourless, defect free crystal was obtained in the beaker and taken for recrystallization process.

Again the saturated Mannitol solution was prepared in accordance with solubility (18 g/100 ml in methanol). The fine seed crystal was hanged in mother solution and Mannitol crystal of size 14×8×10 mm^3 was obtained within 15 days. The Mannitol single crystals are irradiated using a Gamma chamber. Samples with size 1 × 1.2 cm^2 were used for measurement and the dose rate 2 and 4 kGy were used. The parameters used for gamma irradiation is listed in **Table 1**. The pure, 2 and 4 kGy dose of irradiated

Mannitol single crystal are shown in **Fig. 1(a), Fig. 1 (b)** and **Fig. 1 (c)** respectively.

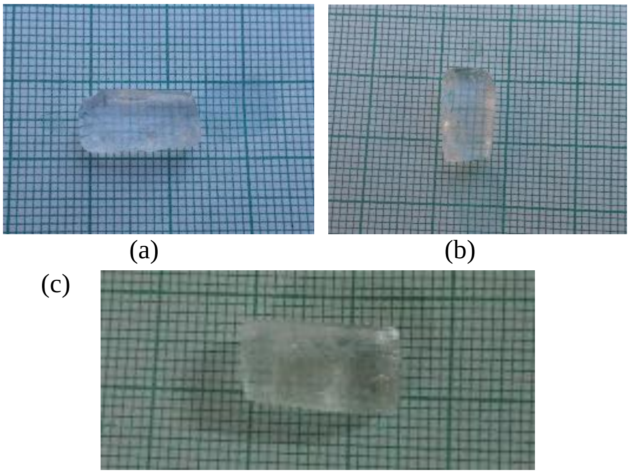

Fig. 1. (a) As grown Mannitol single; (b) Irradiated (2 kGy dose) Mannitol crystal single crystal; (c) Irradiated (4 kGy dose) Mannitol single crystal.

Table 1. The essential specifications of Gamma ray chamber used for the experiment.

Maximum Co-60 source capacity	518 TBq (14,000 Ci)
Dose rate at maximum capacity	9.5 kGy/hy (0.95 megarad/hr)
Dose rate uniformity	Radial +25% or better and axial -25% or better
Irradiation volume	5000 cc
Shielding material	Lead & Stainless
Minimum irradiation time	6 seconds

Results and discussion

Single crystal X-ray diffraction analysis

The lattice parameters of the pure and irradiated Mannitol single crystal were carried out using single crystal X-ray diffractometer (Model:ENRAF NONIUS CAD4/MACH3) and the results confirmed that the pure and gamma irradiated Mannitol single crystal belong to orthorhombic crystal system. After irradiation, the crystal structure remains same with a small change in its lattice parameters. The lattice parameters of pure and gamma irradiated Mannitol single crystals are listed in **Table 2**.

Table 2. The lattice parameters of pure and irradiated Mannitol single crystal.

Sample	a (Å)	b (Å)	c (Å)	α (°)	β (°)	γ (°)	Volume (Å^3)	Structure
Pure Mannitol	5.570	8.700	16.881	90	90	90	817	Orthorhombic
2 kGy	5.429	8.582	16.720	90	90	90	779	Orthorhombic
4 kGy	5.284	8.420	16.648	90	90	90	740	Orthorhombic

Optical transmittance analysis

UV-Vis transmittance spectrum of Pure and irradiated Mannitol crystals were recorded in the wavelength range 200-900 nm at room temperature using T90+PG spectrophotometer. The recorded UV-transmittance spectra for pure and irradiated Mannitol crystals are shown in **Fig. 2**.

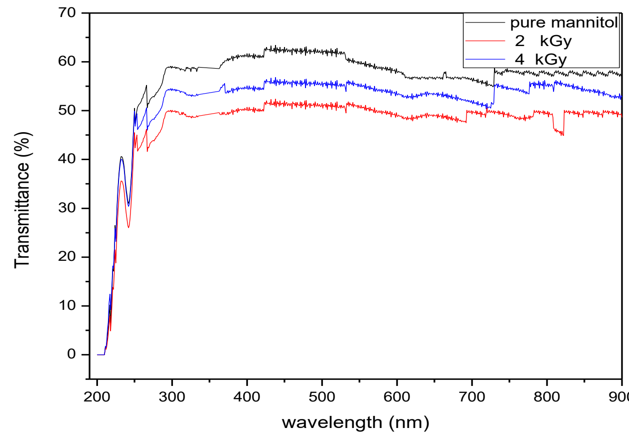

Fig. 2. UV-Visible spectrum of pure and irradiated mannital single crystal.

It is observed that the cut-off wavelength is 210, 209 and 207 nm for pure, 2 and 4 kGy dose of Gamma irradiated Mannitol crystals respectively.

It is noted that there is no significant absorption in the entire visible region, which enables it to be a potential candidate for optoelectronic applications and it is observed that transmittances percentage of irradiated Mannitol crystals decrease on increasing the dosage.

There is no systematic behaviour in the optical transmittance of Pure and irradiated Mannitol single crystals. The absorption increases by increasing dose due to the formation of additional defect centers. The concentration of defects is increased by ion influence which causes increase in the absorption, which may be attributed to the structural rearrangements created [**9-10**].

High resolution X-ray diffraction analysis

The crystalline perfection of the Pure and irradiated Mannitol single crystals were subjected to high-resolution X-ray diffraction (HRXRD) studies using a multi-crystal X-ray diffractometer. **Fig. 3** shows the high-resolution rocking/diffraction curves (DCs) of Pure Mannitol crystals using (1 0 0) diffracting planes in symmetrical Bragg geometry. [**11**].

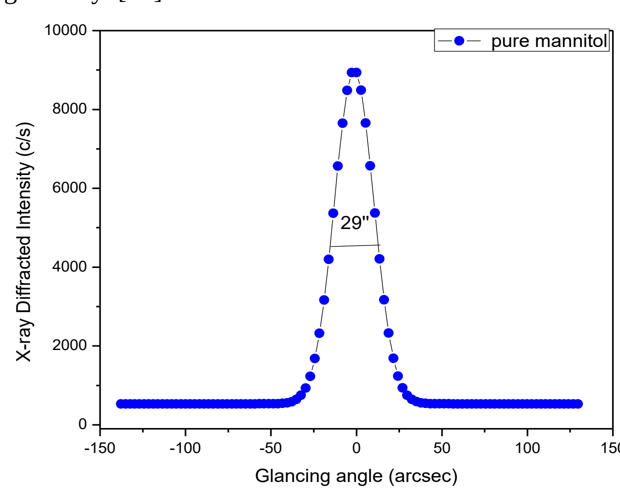

Fig. 3. HRXRD curve for pure (2 kGy) Mannitol single crystal.

The non-crystallized solute atoms or uneven surface of the crystal was removed by lapped and chemical etching using water and acetone mixture in 1:2 volume ratios.

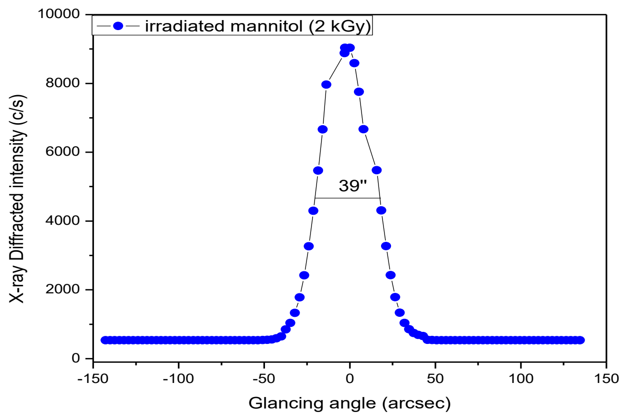

Fig. 4. HRXRD curve for irradiated Mannitol single crystal.

Fig. 4 shows the diffracted curve for 2 kGy dose of gamma irradiated Mannitol single crystal. The diffraction curve contain a single peak and indicates that the specimen is free from structural grain boundaries. The curves are sharp with full width at half maximum (FWHM) of 29 arcsec which is expected for an ideally perfect crystal from the plane wave dynamical theory of X-ray diffraction. Though the specimen contain very low angle boundaries, the grown crystals have good perfection. It is due the solvent molecules or thermal fluctuations during the growth process and such defects may not influence the NLO properties of the crystals.

However, a quantitative analysis of such unavoidable defects is of great importance, particularly in the case of phase matching application. The asymmetry is clearly observed in the negative direction which indicates that the crystal contains vacancy-type defects which may be attributed to the formation of points /clusters defects.

Fig. 5 shows that diffracted curve for 4 kGy dose of gamma irradiated Mannitol single crystals with a full width half maximum (FWHM) of 42 arcsec. From the studies, it is observed that the curve is asymmetry in the asymmetric positive direction, which indicates that the crystal is having interstitial type defects. The FWHM increases with increasing dose of gamma radiation. The intensity of the rocking curve slightly decreases as the dose of gamma radiation is increased, which indicates the presence of defects.

Second Harmonic Generation (SHG) measurement

The second harmonic generation efficiency of Pure and irradiated Mannitol crystals were measured using Q-switched Nd:YAG laser beam of wavelength 1064 nm. The 5 mJ/pulse of laser beam was irradiated on the capillary tube, which contained non-irradiated and irradiated Mannitol crystal powders and the green signal emerged from the capillary tube. The output SHG intensity was made to fall on the high sensitive photo multiplier tube.

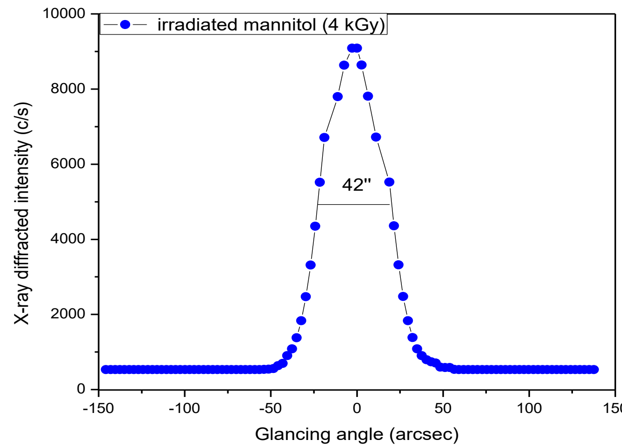

Fig. 5. HRXRD curve for irradiated (4 kGy) Mannitol single crystal.

The corresponding electrical signal was recorded and similar procedure was followed for different particle size of the powdered samples. The intensity of the second harmonic generation output as a function of particle size was measured and is depicted in **Fig. 6**. It is observed that the SHG output increases with respect to the range of the particle sizes (r), all the particles in the laser beam are effectively phase-matched while the number of particles in the light path decreases inversely with r. As r becomes larger than the average coherence length, the SHG output reaches saturation, indicating the phase matchable character of all samples.

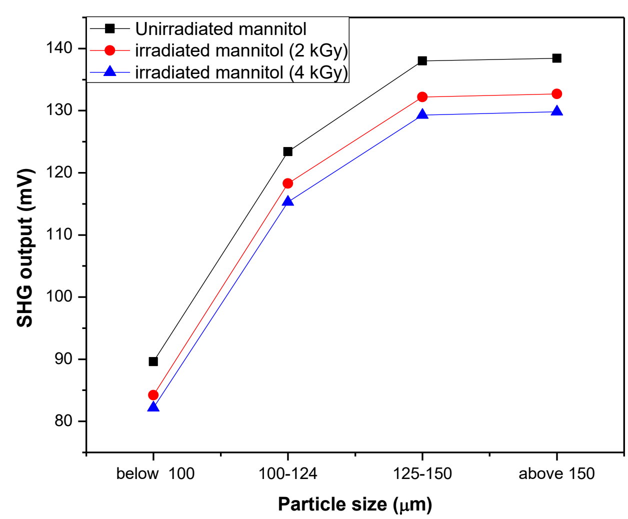

Fig. 6. SHG intensity versus particle sizes for pure and irradiated Mannitol single crystal.

The irradiated and nonradiated Mannitol crystals were illuminated by laser beam. The green light emerged from the crystal and output SHG signal was recorded. The plot between the wavelength and SHG intensity was obtained and shown in **Fig. 7**. From the measurement, the SHG output decreases with increasing dose of gamma radiation. So, generally, the sensitivity to the gamma radiation has an inverse behaviour with respect to the optical SHG. This fact indicate that the defects stimulated by the gamma irradiation have different influence on occurrence of the local non-centro symmetry causing the SHG and decreasing laser damage threshold [**12**].

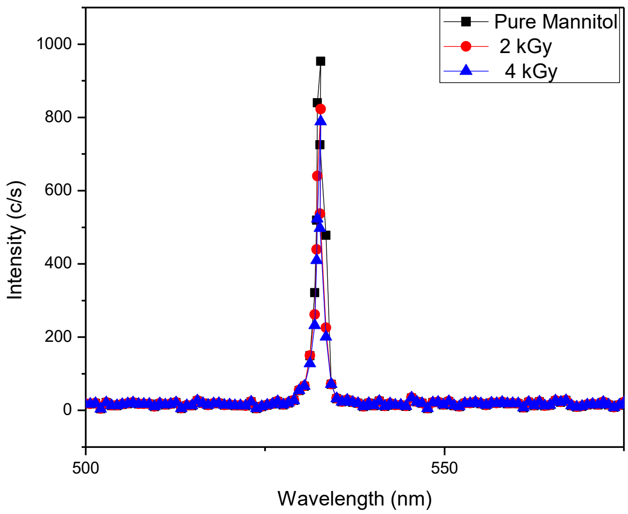

Fig. 7. SHG intensity for pure and irradiated Mannitol single crystal.

Laser damage threshold study

A Q-switched Nd: YAG Innolas laser of pulse width 7 ns and 10 Hz repetition rate operating in TEM00 mode is used as the source. The sample is mounted on an X–Y translator which facilitates in bringing different areas of the sample for exposure precisely. For surface damage, the sample is placed at the focus of a plano-convex lens of focal length 80 mm [**13**].

The energy density is calculated by taking the ratio of input energy and area of the crystal exposed to laser irradiation which is expressed in mJ cm^{-2}.

The surface damage threshold of the crystal was calculated using the expression;

$$\text{Power density } (P_d) = E / \tau\pi r^2 \qquad (W/cm^2)$$

where E is the energy (mJ), τ is the pulse width (ns) and r is the radius of the beam spot (mm). The laser induced damage threshold of nonirradiated and irradiated Mannitol single crystals are listed in **Table 3**.

Table 3. The laser damage threshold of nonirradiated and radiated manitol single crystal.

Sample	Spot radius mm	Mean time Ns	Input energy mJ	Power density GW/cm^2
Unirradiated Mannitol	0.5	10	56	7.13
Irradiated mannitol (2 kGy)	0.5	10	49	6.2
Irradiated mannitol (4 kGy)	0.5	10	44	5.6

From the measurement, the laser damage threshold values are reduced when increasing the dose of gamma radiation. It is due to defects in the irradiated materials produced by gamma radiation and confirmed in the SHG test.

Conclusion

The Mannitol single crystal was grown by solution growth. The gamma radiation was irradiated on Mannitol single crystal using gamma ray chamber. The lattice parameters of irradiated Mannitol was compared with nonirradiated Mannitol and its crystal structures were identified by single crystal X-ray diffraction analysis. The structural perfection of nonirradiated and irradiated Mannitol were studied. The FWHM of diffracted curves were increased with respect to increase in the dose of gamma radiation.

The transmittance percentage of the nonirradiated and irradiated Mannitol were varied and no addition peak was observed in visible region using UV-Visible spectroscopic analysis. The refractive index of nonirradiated and irradiated Mannitol single crystal were measured and refractive index of irradiated single crystal was altered due to defects created by gamma radiation.

The second harmonic generation intensity of irradiated Mannitol was decreased when increasing the dose of gamma radiation. It is due to decrease of laser damage threshold and it was verified using Nd:YAG laser.

Keywords

Gamma irradiation, X-ray diffraction analysis, single crystal, second harmonic generation, dielectric studies.

References

1. Vaddigiri, A.; Potter, K. S.; Thomes, W. J.; Meister, D. C.; *IEEE Transactions on Nuclear Science*, **2006**, *53*, 3882.
2. Matkovskii, A.; Potera, P.; Sugak, D.; Zhydachevskii, Y.; Pankratov, V.; Millers, D.; Grigorjeva, L.; Pracka, I.; Lukasiewicz, T.; *Cryst. Res. Technol.*, **2003**, *38*, 388.
3. Vijayan, N.; Bhagavannarayana, G.; Ramesh Babu, R.; Gopalakrishnan, R.; *Cryst. Growth Des.*, **2006**, *6*, 1542.
4. Narasimha, S.P.; Upendra, N.S.; Darrel, J.A.; "All solid state UV transmitter development for ozone sensing application" J. Opt Proceedings of the 15th Coherent Laser Radar Conference, NASA Langley Research Center, **2009**, 22-26.
5. Dong, Y.; Xu, J.; Zhou; *Sol Stat. Comm.*, **2007**, *141*, 105.
6. Roth, U.; Trobs, M.; Graf, T.; *Appl. Opt.*, **2002**, *41*, 464.
7. EL-Mallawan, R.; EL-Rahamani, A.; Abousehl, Y. A.; Yousef, E.; *Mater. Chem. Phys.*, **1998**, *161*, 52.
8. Ubizskii, S.B.; Matkovskii A.O.; Mironova-Ulmane, N.; *Phys. Stat. Sol. (A)*, **2000**, *177*, 349.
9. Kanagasekaran, T.; Mythili, P.; Kumar, B.; *Nucl. Instr. Meth. Phys. Res. B.*, **2010**, *268*, 36.
10. Virk, H.S.; Chandi, P.S.; Srivastava, A.K.; *Nucl. Instr. Meth. Phys. Res. B.*, **2001**, *183*, 329.
11. Batterman, B. W.; Cole, H.; *Rev. Mod. Phys.*, **1964**, *36*, 681.
12. Vijayalakshmi, R.; Naseema, K.; *Pramama J. Phys.*, **2010**, *75*, 513.
13. Vijayan, N.; Bhagavannarayana, G.; Kanagasekaran, T.; Ramesh Babu, R.; Gopalakrishnan, R.; Ramasamy, P.; *Cryst. Res. Technol.*, **2006**, *4*, 784.